EUROPEAN ORGANIZATION FOR NUCLEAR RESEARCH

LEP2FF/01-02

ALEPH 2001-076 PHYSIC 2001-026
DELPHI 2001-128 PHYS 904
L3 note 2712
OPAL TN704

28 September 2001

Combination of the LEP II $f\bar{f}$ Results

LEPEWWG $f\bar{f}$ Subgroup

Members :

C. Geweniger, C. Goy, M-N Minard
M. Elsing, J. Holt, W. Liebig, P. Renton
S. Blyth, D. Bourilkov, S. Riemann, S. Wynhoff
M. Kobel, S. Marcellini, K. Sachs, P. Ward

Abstract

Preliminary combinations of measurements of the 4 LEP collaborations of the process $e^+e^- \to f\bar{f}$ at LEP-II are presented, using data from the full LEP-II data set where available. Cross-sections and forward-backward asymmetry measurements are combined for the full LEP-II data set. Combined differential cross-sections $\frac{d\sigma}{d\cos\theta}$ for muon-pair and tau-pair final states are presented. Measurements of the production of heavy flavours are combined. The combined results are interpreted in terms of contact interactions and the exchange of Z' bosons.

Results Prepared for Summer Conferences 2001

1 Introduction

Since the start of the LEP-II program LEP has delivered collisions at energies from ~ 130 GeV to ~ 209 GeV. The 4 LEP experiments have made measurements on the $e^+e^- \to f\bar{f}$ process over this range of energies, and a preliminary combination of these data is discussed in this note.

In the years 1995 through 1999 LEP delivered luminosity at a number of distinct centre-of-mass energy points. In 2000 most of the luminosity was delivered close to 2 distinct energies, but there was also a significant fraction of the luminosity delivered in, more-or-less, a continuum of energies. To facilitate the combination of the data, the 4 LEP experiments all divided the data they collected in 2000 into two energy bins: from 202.5 to 205.5 GeV; and 205.5 GeV and above. The nominal and actual centre-of-mass energies to which the LEP data have been averaged for each year are given in Table 1.

A number of measurements on the process $e^+e^- \to f\bar{f}$ exist and have been combined. The preliminary averages of cross-section and forward-backward asymmetry measurements are discussed in Section 2. The results presented in this section update those presented in [1–4]. Complete results of the combinations are available on the web page [5]. In Section 3 a preliminary average of the differential cross-sections measurements, $\frac{d\sigma}{d\cos\theta}$, for the channels $e^+e^- \to \mu^+\mu^-$ and $e^+e^- \to \tau^+\tau^-$ is presented. In Section 4 a preliminary combination of the heavy flavour results R_b, R_c, $A_{FB}^{b\bar{b}}$ and $A_{FB}^{c\bar{c}}$ from LEP-II is presented. In Section 5 the combined results are interpreted in terms of contact interactions and the exchange of Z' bosons. The results are summarised in section 6.

There are significant changes with respect to results presented in Summer 2000 [2]:

- The method of combining the cross-sections and leptonic forward-backward asymmetries has been improved.
- The combinations have been updated using new data:
  - updated preliminary cross-sections and leptonic forward-backward asymmetries for data taken at centre-of-mass energies of 205 and 207 GeV,
  - new preliminary differential cross-section results for $\mu^+\mu^-$ and $\tau^+\tau^-$ final states,
  - new preliminary heavy flavour results.
- The interpretations have been updated due to the changes in combined LEP results.

2 Averages for Cross-sections and Asymmetries

In this section the results of the preliminary combination of cross-sections and asymmetries are given. The individual experiments' analyses of cross-sections and forward-backward asymmetries are discussed in [6]. The preliminary cross-section and leptonic forward-backward asymmetry results at centre-of-mass energies of 205 and 207 GeV have been updated with respect to [2]. These are now obtained from analyses based on the full set data collected in 2000, giving a significant improvement in the precision of the data at the highest centre-of-mass energy.

Cross-section results were combined for the $e^+e^- \to q\bar{q}$, $e^+e^- \to \mu^+\mu^-$ and $e^+e^- \to \tau^+\tau^-$ channels, forward-backward asymmetry measurements were combined for the $\mu^+\mu^-$ and $\tau^+\tau^-$ final states. The averages were made for the samples of events with high $\sqrt{s'}$.

Individual experiments have their own $f\bar{f}$ signal definitions; corrections were applied to bring the measurements to two common signal definitions:

Year	Nominal Energy GeV	Actual Energy GeV	Luminosity pb^{-1}
1995	130	130.2	~ 3
	136	136.2	~ 3
	133*	133.2	~ 6
1996	161	161.3	~ 10
	172	172.1	~ 10
	167*	166.6	~ 20
1997	130	130.2	~ 2
	136	136.2	~ 2
	183	182.7	~ 50
1998	189	188.6	~ 170
1999	192	191.6	~ 30
	196	195.5	~ 80
	200	199.5	~ 80
	202	201.6	~ 40
2000	205	204.9	~ 80
	207	206.7	~ 140

Table 1: The nominal and actual centre-of-mass energies for data collected during LEP-II operation in each year. The approximate average luminosity analysed per experiment at each energy is also shown. Values marked with a * are average energies for 1995 and 1996 used for heavy flavour results. The data taken at nominal energies of 130 and 136 in 1995 and 1997 are combined by most experiments.

- **Definition 1:** $\sqrt{s'}$ is taken to be the mass of the s-channel propagator, with the $f\bar{f}$ signal being defined by the cut $\sqrt{s'/s} > 0.85$. ISR-FSR photon interference is subtracted to render the propagator mass unambiguous.

- **Definition 2:** For dilepton events, $\sqrt{s'}$ is taken to be the bare invariant mass of the outgoing difermion pair. For hadronic events, it is taken to be the mass of the s-channel propagator. In both cases, ISR-FSR photon interference is included and the signal is defined by the cut $\sqrt{s'/s} > 0.85$. When calculating the contribution to the hadronic cross-section due to ISR-FSR interference, since the propagator mass is ill-defined, it is replaced by the bare $q\bar{q}$ mass.

The corrected measurement M_{LEP} is computed from the experimental measurement M_{exp},

$$M_{LEP} = M_{exp} + (P_{LEP} - P_{exp}),$$

where M_{exp} is the prediction for the measurement obtained for the experiments signal definition and P_{LEP} is the prediction for the common signal definition. The predictions are computed with ZFITTER [7]. The theoretical uncertainties associated with the corrections were obtained by comparing ZFITTER, TOPAZ0 v4.4 [8] and the Monte Carlo generator KK v4.02 [9]. The uncertainties are 0.2% for the hadronic cross-sections, 0.7% for dilepton cross-sections and 0.003 for the leptonic asymmetries [4]. These errors are not included in the combination. Results are presented inside the full 4π angular acceptance. Events containing additional fermion pairs from radiative processes are considered to be signal, providing that the primary pair passes the cut on $\sqrt{s'/s}$ and that the secondary pair has a mass below 70 GeV/c^2.

The average was performed using the best linear unbiased estimator technique [10], which is equivalent to a χ^2 minimisation* For the first time, all the data, from centre-of-mass energies of 130 to 207 GeV were averaged together, taking into account correlation between all LEP-II $e^+e^- \to f\bar{f}$ measurements. Previously, the data were treated as three independent subsamples at (130–183) GeV, (192–202) GeV and the data at (205–207) GeV, ignoring correlations between the subsamples.

Particular care was taken to ensure that the correlations between the hadronic cross-sections were reasonably estimated. As in [2] the errors were broken down into 5 categories

1) The statistical uncertainty plus uncorrelated systematic uncertainties, combined in quadrature.

2) The systematic uncertainty for the final state X which is fully correlated between energy points for that experiment.

3) The systematic uncertainty for experiment Y which is fully correlated between different final states for this energy point.

4) The systematic uncertainty for the final state X which is fully correlated between energy points and between different experiments.

5) The systematic uncertainty which is fully correlated between energy points and between different experiments for all final states.

In previous averages, uncertainties in the hadronic cross-sections arising from fragmentation models and modelling of ISR had been treated as uncorrelated between experiments. However,

*Using the same input data, averages made with the best linear unbiased estimator technique were found to agree with results obtained from the χ^2 minimisation technique used in [2].

although there are some differences between the models used and the methods of evaluating the errors, there are significant common elements in the estimation of these sources of uncertainty between the experiments. For the average reported here, these errors were treated as fully correlated between energy points and experiments.

Table 2 gives the averaged cross-sections and forward-backward asymmetries for all energies for definition 1. The differences in the results obtained using definition 2 are also given.

The χ^2 per degree of freedom for the average of the LEP-II $f\bar{f}$ data is 170/180. The correlations are rather small, with the largest components at any given pair of energies being between the hadronic cross-sections. The other off-diagonal terms in the correlation matrix are smaller than 10%. The correlation matrix between the averaged hadronic cross-sections at different centre-of-mass energies is given in Table 3.

Differences in the results with respect to previous combinations at centre-of-mass energies from 130–202 GeV [2,3] arise mainly from the introduction of correlations between measurements which were previously uncorrelated, and the improved treatment of the correlations themselves.

Figures 1 and 2 show the LEP averaged cross-sections and asymmetries, respectively, as a function of the centre-of-mass energy, together with the SM predictions. There is good agreement between the SM expectations and the measurements of the individual experiments and the combined averages. The cross-sections for hadronic final states at most of the energy points are somewhat above the SM expectations. Taking into account the correlations between the data points and also assigning an error of $\pm 0.26\%$ [11] on the absolute SM predictions, the difference of the cross-section from the SM expectations averaged over all energies is approximately a 1.8 standard deviation excess. It is concluded that there is no significant evidence in the results of the combinations for physics beyond the SM in the process $e^+e^- \to f\bar{f}$.

3 Averages for Differential Cross-sections

The LEP experiments have measured the differential cross-section, $\frac{d\sigma}{d\cos\theta}$, for the $e^+e^- \to \mu^+\mu^-$ and $e^+e^- \to \tau^+\tau^-$ channels for samples of events with $\sqrt{s'/s} > 0.85$. A preliminary combination of these results has been made using a χ^2 fit to the measured differential cross sections, using the expected error on the differential cross sections, computed from the expected cross sections and the expected numbers of events in each experiment. Using a Monte Carlo simulation it has been shown that this method provides a good approximation to the exact likelihood method based on Poisson statistics [2].

The combination included data from 183 to 207 GeV, but not all experiments provided data at all energies. Since [2], new, preliminary, results for centre-of-mass energies of 205 and 207 GeV have been made available by all experiments. In addition, new, preliminary, results for $e^+e^- \to \mu^+\mu^-$ at energies from 192–202 GeV from L3 have been made available. The data used in the combination are summarised in Table 4.

Each experiment's data were binned in 10 bins of $\cos\theta$ at each energy, using their own signal definiton. The scattering angle, θ, is the angle of the negative lepton with respect to the incoming electron direction in the lab coordinate system. The outer acceptances of the most forward and most backward bins for which the four experiments have presented their data were different. This was accounted for as part of the correction to a common signal definition. The ranges in $\cos\theta$ for the measurements of the individual experiments and the average are given in Table 5. The signal definition used corresponded to definition 1 of Section 2.

Correlated small systematic errors between different experiments, channels and energies,

$\sqrt{s}$ (GeV)	Quantity	Average value	SM	Δ
130	$\sigma(q\overline{q})$ [pb]	82.124±2.232	82.803	-0.251
	$\sigma(\mu^+\mu^-)$ [pb]	8.620±0.682	8.439	-0.331
	$\sigma(\tau^+\tau^-)$ [pb]	9.036±0.930	8.435	-0.108
	$A_{fb}(\mu^+\mu^-)$	0.693±0.060	0.705	0.012
	$A_{fb}(\tau^+\tau^-)$	0.663±0.076	0.704	0.012
136	$\sigma(q\overline{q})$ [pb]	66.724±1.974	66.596	-0.224
	$\sigma(\mu^+\mu^-)$ [pb]	8.276±0.677	7.281	-0.280
	$\sigma(\tau^+\tau^-)$ [pb]	7.086±0.820	7.279	-0.091
	$A_{fb}(\mu^+\mu^-)$	0.707±0.060	0.684	0.013
	$A_{fb}(\tau^+\tau^-)$	0.752±0.088	0.683	0.014
161	$\sigma(q\overline{q})$ [pb]	37.014±1.074	35.247	-0.143
	$\sigma(\mu^+\mu^-)$ [pb]	4.608±0.364	4.613	-0.178
	$\sigma(\tau^+\tau^-)$ [pb]	5.673±0.545	4.613	-0.061
	$A_{fb}(\mu^+\mu^-)$	0.537±0.067	0.609	0.017
	$A_{fb}(\tau^+\tau^-)$	0.646±0.077	0.609	0.016
172	$\sigma(q\overline{q})$ [pb]	29.262±0.989	28.738	-0.124
	$\sigma(\mu^+\mu^-)$ [pb]	3.571±0.317	3.952	-0.157
	$\sigma(\tau^+\tau^-)$ [pb]	4.013±0.450	3.951	-0.054
	$A_{fb}(\mu^+\mu^-)$	0.674±0.077	0.591	0.018
	$A_{fb}(\tau^+\tau^-)$	0.342±0.094	0.591	0.017
183	$\sigma(q\overline{q})$ [pb]	24.609±0.426	24.200	-0.109
	$\sigma(\mu^+\mu^-)$ [pb]	3.490±0.147	3.446	-0.139
	$\sigma(\tau^+\tau^-)$ [pb]	3.375±0.174	3.446	-0.050
	$A_{fb}(\mu^+\mu^-)$	0.559±0.035	0.576	0.018
	$A_{fb}(\tau^+\tau^-)$	0.608±0.045	0.576	0.018
189	$\sigma(q\overline{q})$ [pb]	22.446±0.257	22.156	-0.101
	$\sigma(\mu^+\mu^-)$ [pb]	3.116±0.077	3.207	-0.131
	$\sigma(\tau^+\tau^-)$ [pb]	3.121±0.099	3.207	-0.048
	$A_{fb}(\mu^+\mu^-)$	0.566±0.021	0.569	0.019
	$A_{fb}(\tau^+\tau^-)$	0.584±0.028	0.569	0.018
192	$\sigma(q\overline{q})$ [pb]	22.291±0.523	21.237	-0.098
	$\sigma(\mu^+\mu^-)$ [pb]	2.943±0.175	3.097	-0.127
	$\sigma(\tau^+\tau^-)$ [pb]	2.832±0.216	3.097	-0.047
	$A_{fb}(\mu^+\mu^-)$	0.540±0.052	0.566	0.019
	$A_{fb}(\tau^+\tau^-)$	0.614±0.070	0.566	0.019
196	$\sigma(q\overline{q})$ [pb]	20.729±0.338	20.127	-0.094
	$\sigma(\mu^+\mu^-)$ [pb]	2.967±0.106	2.962	-0.123
	$\sigma(\tau^+\tau^-)$ [pb]	2.984±0.138	2.962	-0.045
	$A_{fb}(\mu^+\mu^-)$	0.580±0.031	0.562	0.019
	$A_{fb}(\tau^+\tau^-)$	0.493±0.045	0.562	0.019
200	$\sigma(q\overline{q})$ [pb]	19.372±0.319	19.085	-0.090
	$\sigma(\mu^+\mu^-)$ [pb]	3.040±0.104	2.834	-0.118
	$\sigma(\tau^+\tau^-)$ [pb]	2.966±0.134	2.833	-0.044
	$A_{fb}(\mu^+\mu^-)$	0.518±0.031	0.558	0.019
	$A_{fb}(\tau^+\tau^-)$	0.549±0.043	0.558	0.019
202	$\sigma(q\overline{q})$ [pb]	19.278±0.430	18.572	-0.088
	$\sigma(\mu^+\mu^-)$ [pb]	2.621±0.139	2.770	-0.116
	$\sigma(\tau^+\tau^-)$ [pb]	2.777±0.183	2.769	-0.044
	$A_{fb}(\mu^+\mu^-)$	0.543±0.048	0.556	0.020
	$A_{fb}(\tau^+\tau^-)$	0.583±0.060	0.556	0.019
205	$\sigma(q\overline{q})$ [pb]	18.119±0.316	17.811	-0.085
	$\sigma(\mu^+\mu^-)$ [pb]	2.449±0.100	2.674	-0.112
	$\sigma(\tau^+\tau^-)$ [pb]	2.705±0.129	2.673	-0.042
	$A_{fb}(\mu^+\mu^-)$	0.558±0.036	0.553	0.020
	$A_{fb}(\tau^+\tau^-)$	0.565±0.044	0.553	0.019
207	$\sigma(q\overline{q})$ [pb]	17.423±0.263	17.418	-0.083
	$\sigma(\mu^+\mu^-)$ [pb]	2.613±0.088	2.623	-0.111
	$\sigma(\tau^+\tau^-)$ [pb]	2.528±0.108	2.623	-0.042
	$A_{fb}(\mu^+\mu^-)$	0.540±0.029	0.552	0.020
	$A_{fb}(\tau^+\tau^-)$	0.561±0.038	0.551	0.019

Table 2: Preliminary combined LEP results for $e^+e^- \to f\overline{f}$. All the results correspond to the signal definition 1. The Standard Model predictions are from ZFITTER [7]. The difference, Δ, in the averages for the measurments for definition 2 relative to definition 1 are given in the final column. The quoted uncertainties do not include the theoretical uncertainties on the corrections discussed in the text.

$\sqrt{s}$ GeV)	130	136	161	172	183	189	192	196	200	202	205	207
130	1.000	0.075	0.085	0.076	0.121	0.151	0.084	0.116	0.131	0.091	0.137	0.160
136		1.000	0.079	0.071	0.112	0.140	0.078	0.107	0.121	0.084	0.127	0.148
161			1.000	0.082	0.128	0.162	0.089	0.123	0.139	0.097	0.144	0.167
172				1.000	0.114	0.145	0.080	0.110	0.125	0.087	0.130	0.150
183					1.000	0.237	0.130	0.179	0.203	0.139	0.208	0.242
189						1.000	0.173	0.236	0.270	0.184	0.266	0.307
192							1.000	0.136	0.156	0.106	0.151	0.173
196								1.000	0.212	0.145	0.207	0.238
200									1.000	0.166	0.236	0.271
202										1.000	0.162	0.185
205											1.000	0.282
207												1.000

Table 3: The correlation coefficients between averaged hadronic cross-sections at different energies.

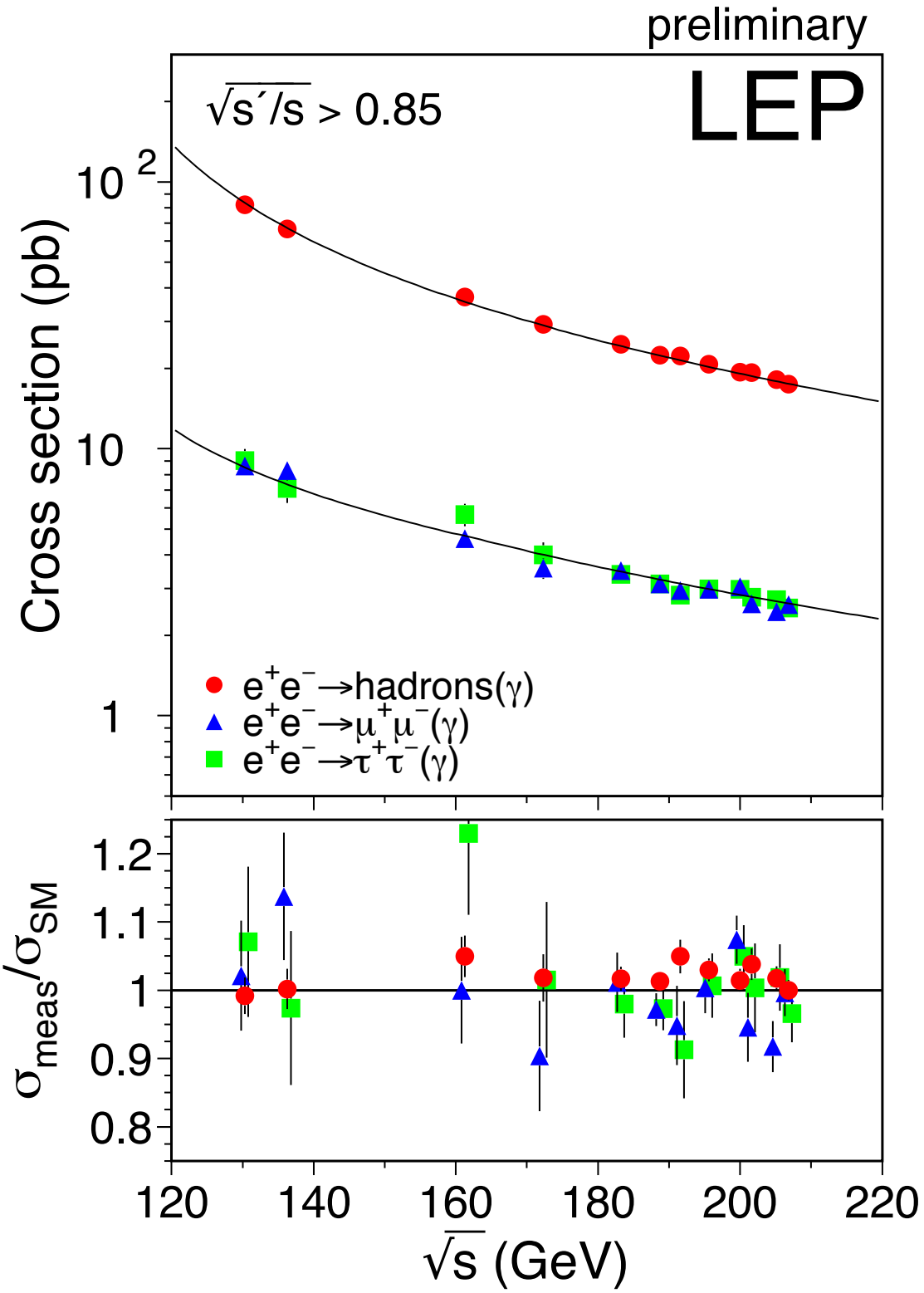

Figure 1: Preliminary combined LEP results on the cross-sections for $q\overline{q}$, $\mu^+\mu^-$ and $\tau^+\tau^-$ final states, as a function of centre-of-mass energy. The expectations of the SM, computed with ZFITTER [7], are shown as curves. The lower plot shows the ratio of the data divided by the SM.

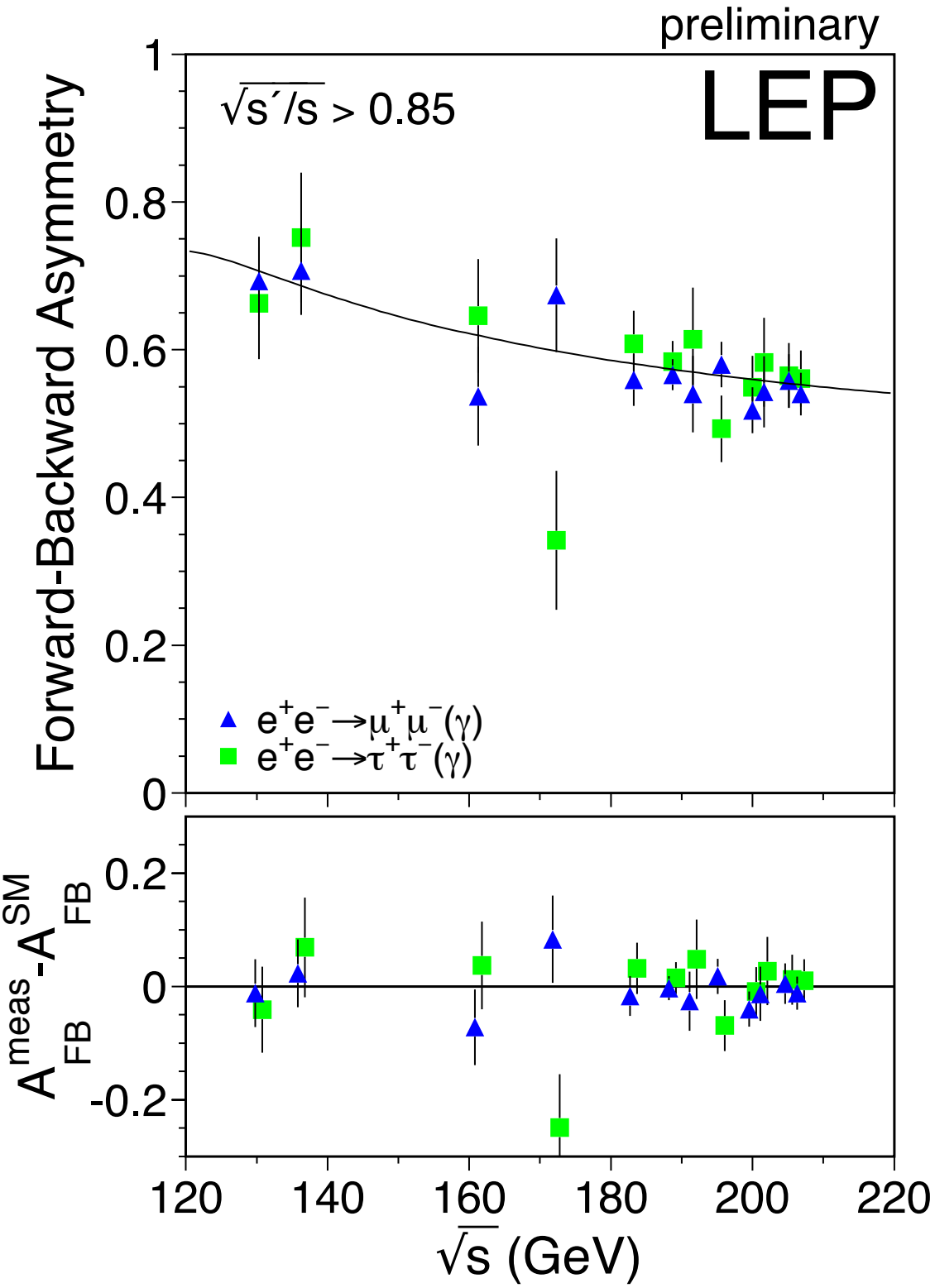

Figure 2: Preliminary combined LEP results on the forward-backward asymmetry for $\mu^+\mu^-$ and $\tau^+\tau^-$ final states as a function of centre-of-mass energy. The expectations of the SM computed with ZFITTER [7], are shown as curves. The lower plot shows differences between the data and the SM.

	$e^+e^- \to \mu^+\mu^-$				$e^+e^- \to \tau^+\tau^-$			
$\sqrt{s}$(GeV)	A	D	L	O	A	D	L	O
183	-	F	-	F	-	F	-	F
189	P	F	F	F	P	F	F	F
192–202	P	P	P	P	P	P	-	P
205–207	P	P	P	P	P	P	-	P

Table 4: Differential cross-section data provided by the LEP collaborations (ALEPH, DELPHI, L3 and OPAL) for $e^+e^- \to \mu^+\mu^-$ and $e^+e^- \to \tau^+\tau^-$ combination at different centre-of-mass energies. Data indicated with F are final, published data. Data marked with P are preliminary. Data marked with a - were not available for combination.

Experiment	$\cos\theta_{min}$	$\cos\theta_{max}$
ALEPH	-0.95	0.95
DELPHI ($e^+e^- \to \mu^+\mu^-$ 183)	-0.94	0.94
DELPHI ($e^+e^- \to \mu^+\mu^-$ 189–207)	-0.97	0.97
DELPHI ($e^+e^- \to \tau^+\tau^-$)	-0.96	0.96
L3	-0.90	0.90
OPAL	-1.00	1.00
Average	-1.00	1.00

Table 5: The acceptances for which experimental data are presented and the acceptance for the LEP average. For DELPHI the acceptance is shown for the different channels and for the muons for different centre of mass energies. For all other experiments the acceptance is the same for muon and tau-lepton channels and for all energies provided.

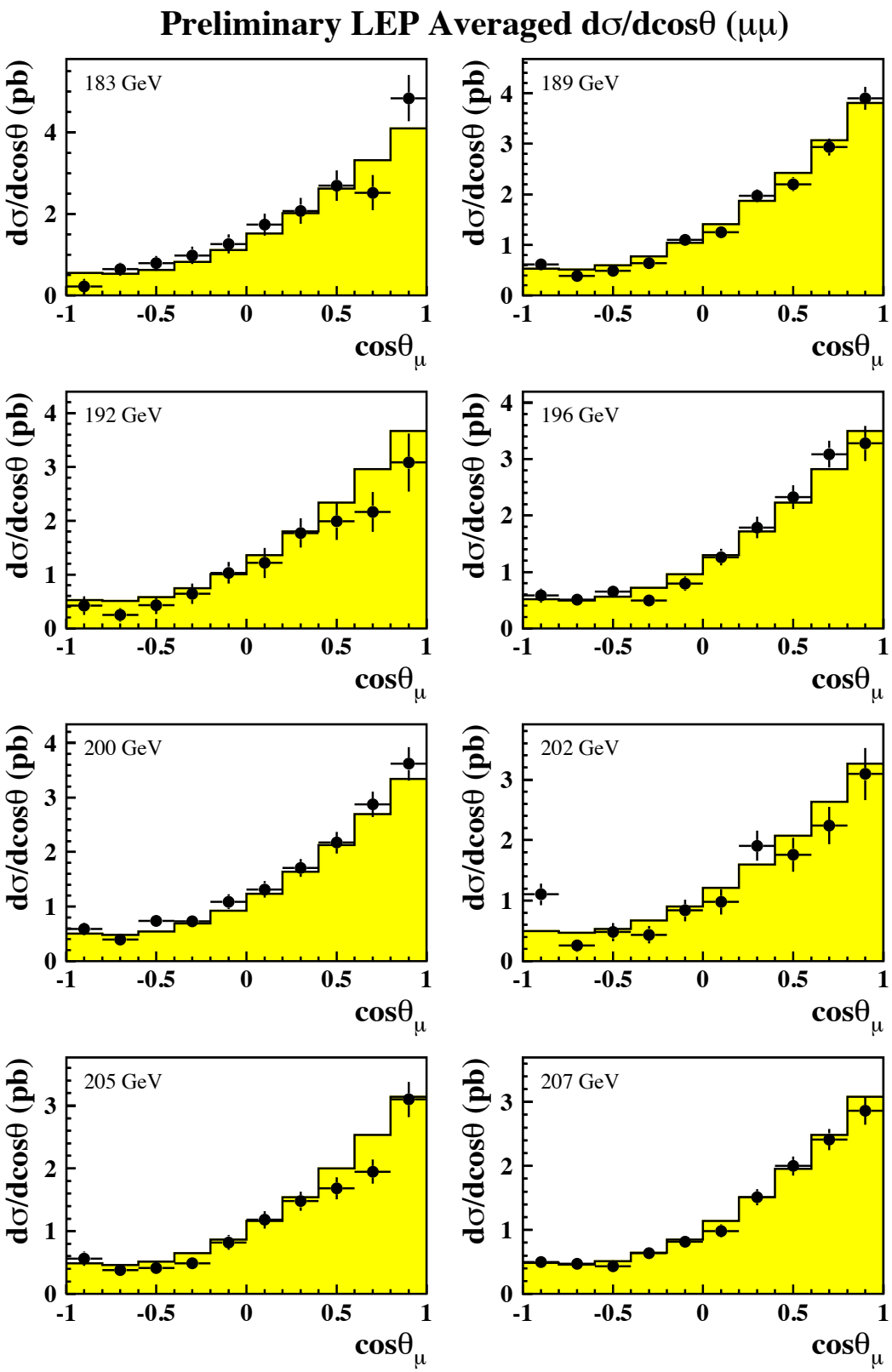

Figure 3: LEP averaged differential cross-sections for $e^+e^- \to \mu^+\mu^-$ at energies of 183–207 GeV. The SM predictions, shown as solid histograms, are computed with ZFITTER [7].

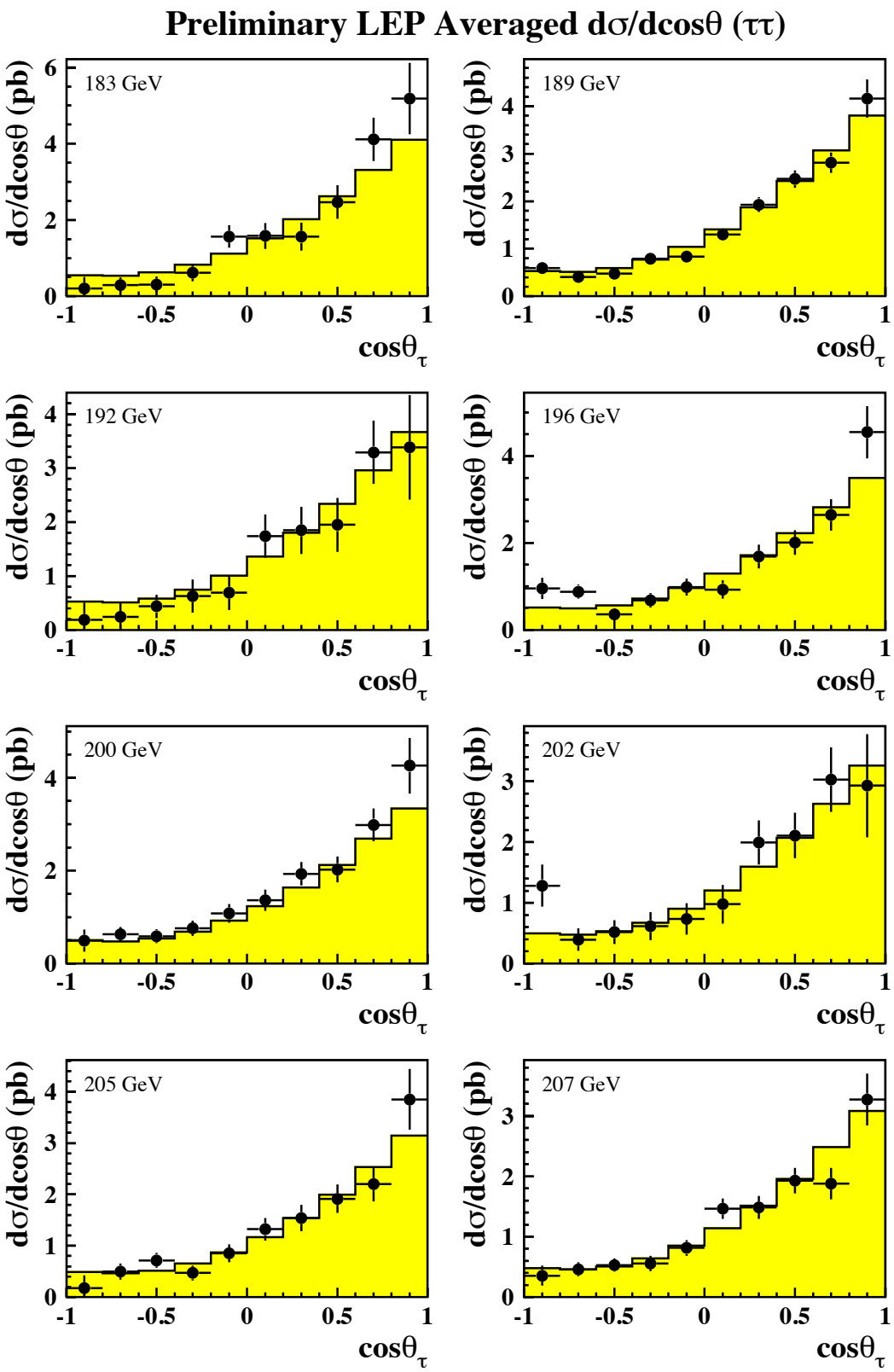

Figure 4: LEP averaged differential cross-sections for $e^+e^- \to \tau^+\tau^-$ at energies of 183–207 GeV. The SM predictions, shown as solid histograms, are computed with ZFITTER [7].

arising from uncertainties on the overall normalisation were considered in the averaging procedure.

Three separate averages were performed; one for 183 and 189 GeV data, one for 192–202 GeV data and for 205 and 207 GeV data. The averages for the 183–189 data set has not been updated with respect to [2]. The results of the averages are shown in Figures 3 and 4.

The correlations between bins in the average are less that 2% of the total error on the averages in each bin. Overall the agreement between the averaged data and the predictions is reasonable, with a χ^2 of 191 for 160 degrees of freedom. At 202 GeV the cross-section in the most backward bin, $-1.00 < \cos\theta < 0.8$, for both muon and tau final states is above the predictions. For the muons the excess in data corresponds to 3.4 standard deviations. For the taus the excess is 2.3 standard deviations, however, for this measurement the individual experiments are somewhat inconsistent, having a χ^2 with respect to the average of 10.5 for 2 degrees of freedom. The data at 202 GeV suffer from rather low delivered luminosity, with less than 4 events expected in each experiment in each channel in this backward $\cos\theta$ bin. The agreement between the data and the predictions in the same $\cos\theta$ bin is better at higher energies.

4 Averages for Heavy Flavour Measurements

This section presents a preliminary combination of both published [12] and preliminary [13] measurements of the ratios[†] R_{b} and R_{c} and the forward-backward asymmetries, $A_{\mathrm{FB}}^{\mathrm{b\overline{b}}}$ and $A_{\mathrm{FB}}^{\mathrm{c\overline{c}}}$, from the LEP collaborations at centre-of-mass energies in the range of 130 to 207 GeV. The averages have been updated with respect to [2]. New, preliminary, results from DELPHI and L3 at centre-of-mass energies of 205 and 207 GeV, based on analyses of the full 2000 data sets are included. New, preliminary, results from ALEPH at lower energies have also been included. Table 6 summarises all the inputs that have been combined.

A common signal definition was defined for all the measurements, requiring:

- an effective centre-of-mass energy $\sqrt{s'} > 0.85\sqrt{s}$
- the inclusion of ISR and FSR photon interference contribution and
- extrapolation to full angular acceptance.

Systematic errors were divided into three categories: uncorrelated errors, errors correlated between the measurements of each experiment, and errors common to all experiments. Full details concerning the combination procedure can be found in [14].

The results of the combination are presented in Table 7 and Figures 5 and 6. The results are consistent with the Standard Model predictions of ZFITTER.

Because of the large correlation (-0.36) with R_{c} at 183 GeV and 189 GeV, the errors on the corresponding measurements of R_{b} receive an additional contribution which is absent at the other energy points. For other energies where there is no measurement of R_{c}, the Standard Model value of R_{c} is used in extracting R_{b} (the error on the Standard Model prediction of R_{c} was estimated to be negligible compared to the other uncertainties on R_{b}).

A list of the error contributions from the combination at 189 GeV is shown in Table 8.

[†]Unlike at LEP-I, R_q^0 is defined as $\frac{\sigma_{\mathrm{q\overline{q}}}}{\sigma_{\mathrm{had}}}$.

$\sqrt{s}$ (GeV)	R_b				R_c				$A_{FB}^{b\bar{b}}$				$A_{FB}^{c\bar{c}}$			
	A	D	L	O	A	D	L	O	A	D	L	O	A	D	L	O
133	F	F	F	F	-	-	-	-	-	F	-	F	-	F	-	F
167	F	F	F	F	-	-	-	-	-	F	-	F	-	F	-	F
183	F	P	F	F	F	-	-	-	F	-	-	F	P	-	-	F
189	P	P	F	F	P	-	-	-	P	P	F	F	P	-	-	F
192 to 202	P	P	P	-	-	-	-	-	P	P	-	-	-	-	-	-
205 and 207	-	P	P	-	-	-	-	-	-	P	-	-	-	-	-	-

Table 6: Data provided by the ALEPH, DELPHI, L3, OPAL collaborations for combination at different centre-of-mass energies. Data indicated with F are final, published data. Data marked with P are preliminary. Data marked with a - were not supplied for combination.

$\sqrt{s}$ (GeV)	R_b	R_c	$A_{FB}^{b\bar{b}}$	$A_{FB}^{c\bar{c}}$
133	0.1811 ± 0.0132	-	0.358 ± 0.251	0.577 ± 0.314
	(0.1853)	-	(0.487)	(0.681)
167	0.1484 ± 0.0127	-	0.620 ± 0.254	0.915 ± 0.344
	(0.1708)	-	(0.561)	(0.671)
183	0.1619 ± 0.0101	0.269 ± 0.043	0.528 ± 0.155	0.658 ± 0.209
	(0.1671)	(0.250)	(0.578)	(0.656)
189	0.1562 ± 0.0065	0.240 ± 0.023	0.488 ± 0.094	0.446 ± 0.151
	(0.1660)	(0.252)	(0.583)	(0.649)
192	0.1541 ± 0.0149	-	0.422 ± 0.267	-
	(0.1655)	-	(0.585)	-
196	0.1542 ± 0.0098	-	0.531 ± 0.151	-
	(0.1648)	-	(0.587)	-
200	0.1675 ± 0.0100	-	0.589 ± 0.150	-
	(0.1642)	-	(0.590)	-
202	0.1635 ± 0.0143	-	0.604 ± 0.241	-
	(0.1638)	-	(0.593)	-
205	0.1588 ± 0.0126	-	0.728 ± 0.258	-
	(0.1634)	-	(0.594)	-
207	0.1680 ± 0.0108	-	0.447 ± 0.200	-
	(0.1632)	-	(0.593)	-

Table 7: Results of the global fit, compared to the Standard Model predictions, computed with ZFITTER [15], for the signal definition in parentheses. Quoted errors represent the statistical and systematic errors added in quadrature. Because of the large correlation with R_c at 183 GeV and 189 GeV, the errors on the corresponding measurements of R_b receive an additional contribution which is absent at the other energy points.

Error list	R_b (189 GeV)	R_c (189 GeV)	$A_{FB}^{b\bar{b}}$ (189 GeV)	$A_{FB}^{c\bar{c}}$ (189 GeV)
statistics	0.00606	0.0179	0.0884	0.1229
internal syst	0.00232	0.0123	0.0296	0.0481
common syst	0.00082	0.0078	0.0138	0.0735
total syst	0.00246	0.0145	0.0327	0.0878
total error	0.00654	0.0231	0.0942	0.1510

Table 8: Error breakdown at 189 GeV.

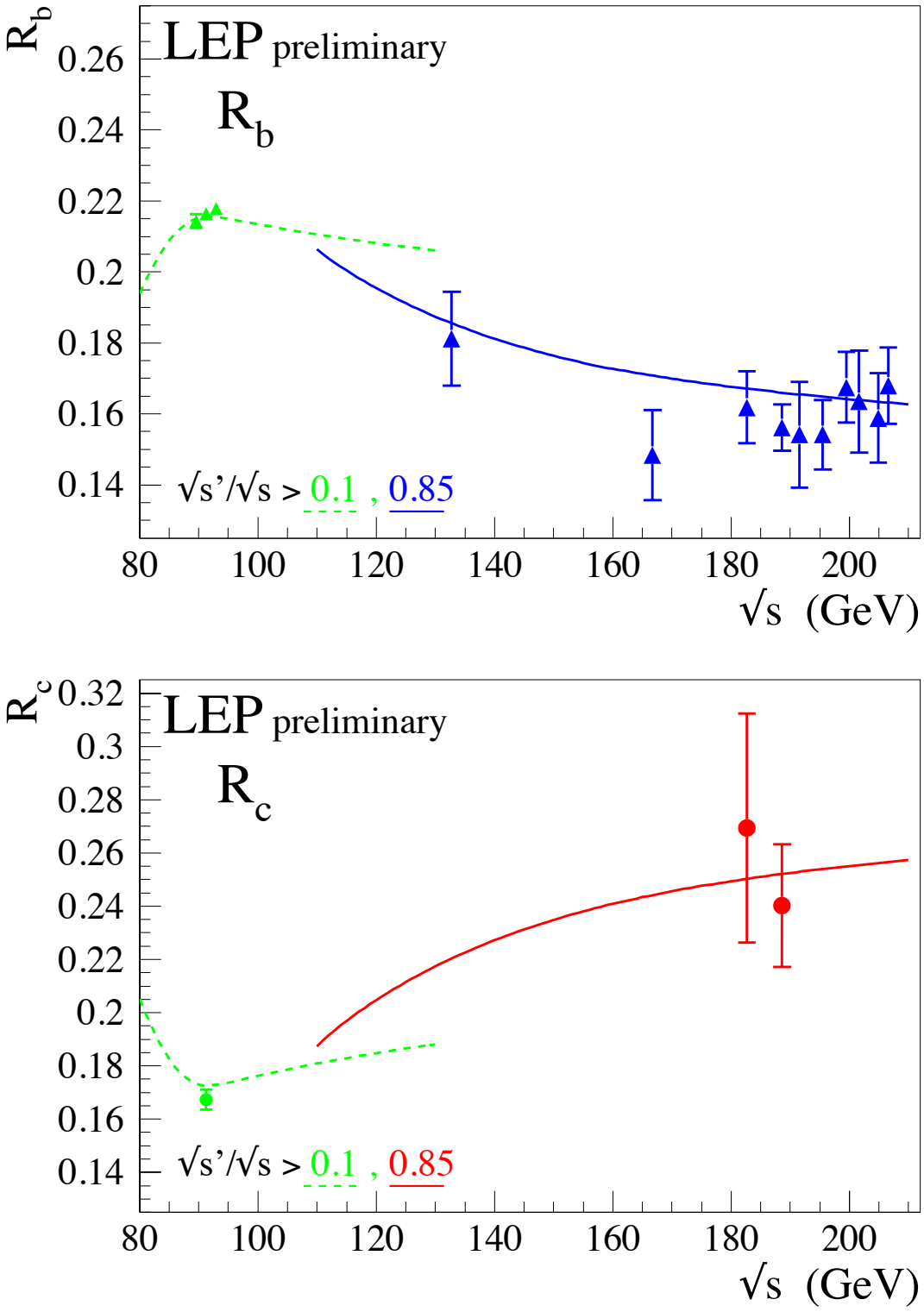

Figure 5: Preliminary combined LEP measurements of R_b and R_c. Solid lines represent the Standard Model prediction for the signal definition and dotted lines the inclusive prediction. Both are computed with ZFITTER[15]. The LEP-I measurements have been taken from [16].

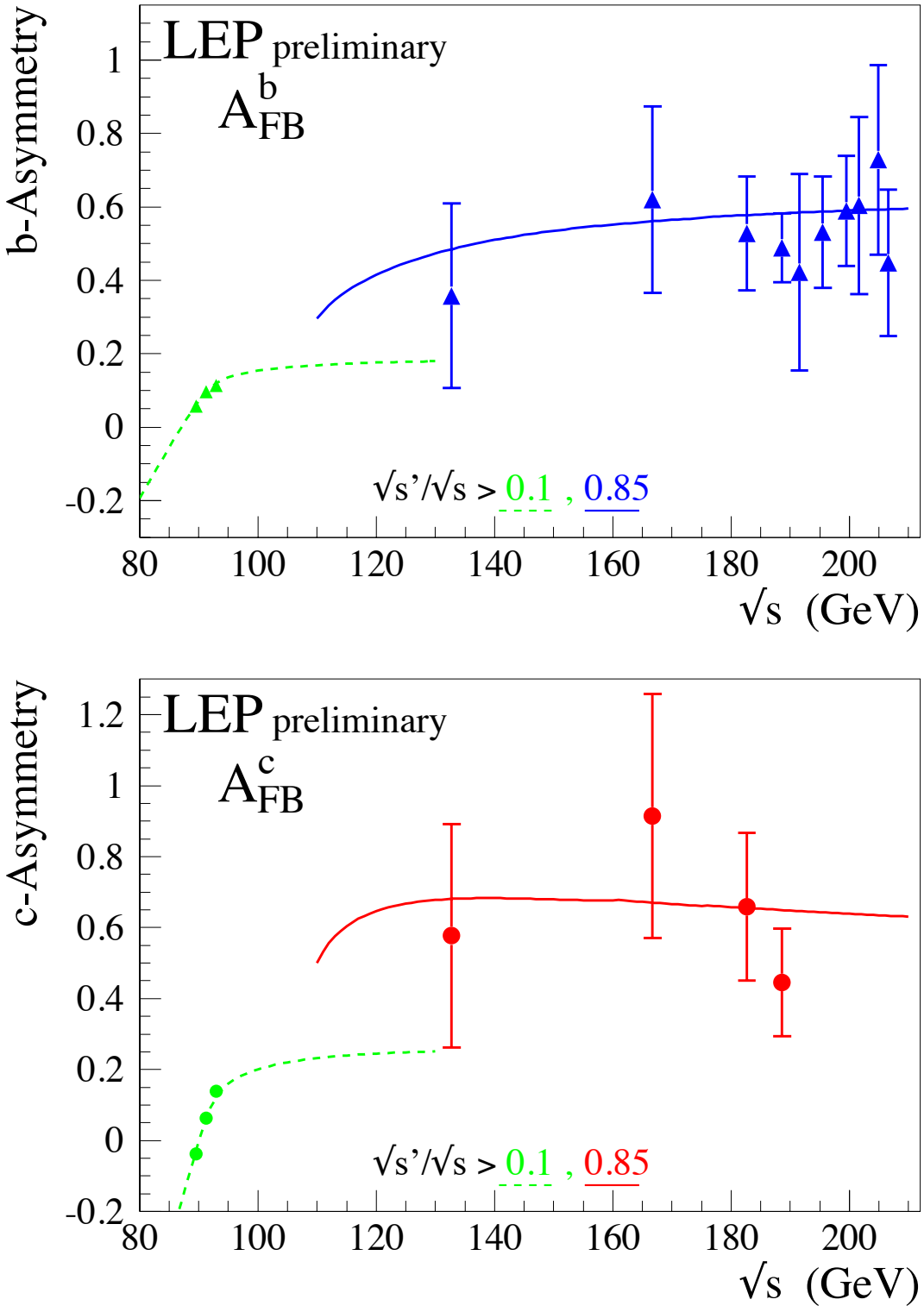

Figure 6: Preliminary combined LEP measurements of the forward–backward asymmetries $A_{FB}^{b\bar{b}}$ and $A_{FB}^{c\bar{c}}$. Solid lines represent the Standard Model prediction for the signal definition and dotted lines the inclusive prediction. Both are computed with ZFITTER [15]. The LEP-I measurements have been taken from [16].

Model	χ	ψ	η	L-R	SSM
$M_{Z'}^{limit}$ (GeV/c^2)	678	463	436	800	1890

Table 9: The 95% confidence level lower limits on the Z′ mass and χ, ψ, η, L-R and SSM models.

5 Interpretation

The combined cross-sections and asymmetries and results on heavy flavour production have been interpreted in a variety of models. The cross-section and asymmetry results have been used to place limits on the mass of a possible additional heavy neutral boson, Z′, in several models. Limits on contact interactions between leptons and on contact interaction between electrons and b and c quarks have been obtained. The results update those provided in [2].

5.1 Models with Z′ Bosons

The combined hadronic and leptonic cross-sections and the leptonic forward-backward asymmetries were used to fit the data to models including an additional, heavy, neutral boson, Z′. The results are updated with respect to those given in [2] due to the updated cross-section and leptonic forward-backward asymmetry results.

Fits were made to the mass of a Z′, $M_{Z'}$, for 4 different models referred to as χ, ψ, η and L-R [17] and for the Sequential Standard Model [18], which proposes the existence of a Z′ with exactly the same coupling to fermions as the standard Z. LEP-II data alone does not significantly constrain the mixing angle between the Z and Z′ fields, $\Theta_{ZZ'}$. However results from a single experiment in which LEP-I data is used in the fit show that the mixing is consistent with zero (see for example [19]). So for these fits $\Theta_{ZZ'}$ was fixed to zero.

No significant evidence was found for the existence of a Z′ boson in any of the models. 95% confidence level lower limits on $M_{Z'}$ were obtained, by integrating the likelihood function[‡]. The lower limits on the Z′ mass are shown in Table 9.

5.2 Contact Interactions between Leptons

The averages of cross-sections and forward-backward asymmetries for muon-pair and tau-lepton pair final states have been used to search for contact interactions between leptons. The results are updated with respect to those given in [2] due to the updated cross-section and leptonic forward-backward asymmetry results.

Following [20], contact interactions are parameterised by an effective Lagrangian, $\mathcal{L}_{\rm eff}$, which is added to the Standard Model Lagrangian and has the form:

$$\mathcal{L}_{\rm eff} = \frac{g^2}{(1+\delta)\Lambda^2} \sum_{i,j=L,R} \eta_{ij} \overline{e}_i \gamma_\mu e_i \overline{f}_j \gamma^\mu f_j,$$

where $g^2/4\pi$ is taken to be 1 by convention, $\delta = 1(0)$ for $f = e$ ($f \neq e$), $\eta_{ij} = \pm 1$ or 0, Λ is the scale of the contact interactions, e_i and f_j are left or right-handed spinors. By assuming different helicity coupling between the initial state and final state currents, a set of different

[‡]To be able to obtain confidence limits from the likelihood function it is necessary to convert the likelihood to a probability density function; this is done by multiplying by a prior probability function. Simply integrating the likelihood is equivalent to multiplying by a uniform prior probability function.

Model	η_{LL}	η_{RR}	η_{LR}	η_{RL}
$LL^{\pm}$	±1	0	0	0
$RR^{\pm}$	0	±1	0	0
$VV^{\pm}$	±1	±1	±1	±1
$AA^{\pm}$	±1	±1	∓1	∓1
$LR^{\pm}$	0	0	±1	0
$RL^{\pm}$	0	0	0	±1
$V0^{\pm}$	±1	±1	0	0
$A0^{\pm}$	0	0	±1	±1

Table 10: Choices of η_{ij} for different contact interaction models

.

models can be defined from this Lagrangian [21], with either constructive (+) or destructive (−) interference between the Standard Model process and the contact interactions. The models and corresponding choices of η_{ij} are given in Table 10. The models LL, RR, VV, AA, LR, RL, V0, A0 are considered here since these models lead to large deviations in the $e^+e^- \to \mu^+\mu^-$ and $e^+e^- \to \tau^+\tau^-$ channels. The total hadronic cross section on its own is not particularly sensitive to contact interactions involving quarks.

For the purpose of fitting contact interaction models to the data, a new parameter $\epsilon = 1/\Lambda^2$ was defined; $\epsilon = 0$ in the limit that there are no contact interactions. This parameter was allowed to take both positive and negative values in the fits. Theoretical uncertainties on the Standard Model predictions were taken from [11].

The values of ϵ extracted for each model were all compatible with the Standard Model expectation $\epsilon = 0$, at the two standard deviation level. These errors on ϵ are typically a factor of two smaller than those obtained from a single LEP experiment with the same data set. The fitted values of ϵ were converted into 95% confidence level lower limits on Λ. The limits are obtained by integrating the likelihood function over the physically allowed values, $\epsilon \geq 0$ for each Λ^+ limit and $\epsilon \leq 0$ for Λ^- limits. The fitted values of ϵ and the extracted limits are shown in Table 11. Figure 7 shows the limits obtained on the scale Λ for the different models assuming universality between contact interactions for $e^+e^- \to \mu^+\mu^-$ and $e^+e^- \to \tau^+\tau^-$.

5.3 Contact Interactions from Heavy Flavour Averages

Limits on contact interactions between electrons and b and c quarks have been obtained. These results are of particular interest since they are inaccessible to $p\bar{p}$ or ep colliders. The formalism for describing contact interactions including heavy flavours is identical to that described above for leptons.

All heavy flavour LEP-II combined results from 133 to 205 GeV given in Table 7 were used as inputs. For the purpose of fitting contact interaction models to the data, R_b and R_c were converted to cross sections $\sigma_{b\bar{b}}$ and $\sigma_{c\bar{c}}$ using the averaged $q\overline{q}$ cross section of section 2 corresponding to signal definition 2. In the calculation of errors, the correlations between R_b, R_c and $\sigma_{q\overline{q}}$ were assumed to be negligible.

The results are updated with respect to those given in [2] due to the updated hadronic cross-sections and heavy flavour results. No evidence for contact interactions between electrons and b and c was found. The fitted values of ϵ and their 68% confidence level uncertainties together with the 95% confidence level lower limit on Λ are shown in Table 12. Figure 8 shows the limits obtained on the scale, Λ, of models with different helicity combinations involved in the

$e^+e^- \to \mu^+\mu^-$			
Model	ϵ (TeV^{-2})	Λ^-(TeV)	Λ^+(TeV)
LL	$-0.0056^{+0.0042}_{-0.0037}$	8.8	14.4
RR	$-0.0060^{+0.0051}_{-0.0046}$	8.4	13.8
VV	$-0.0014^{+0.0016}_{-0.0012}$	15.5	22.2
AA	$-0.0025^{+0.0018}_{-0.0023}$	12.1	20.1
LR	$0.0014^{+0.0043}_{-0.0074}$	7.4	9.3
RL	$0.0014^{+0.0043}_{-0.0074}$	7.4	9.3
V0	$-0.0036^{+0.0032}_{-0.0013}$	12.2	19.9
A0	$0.0008^{+0.0020}_{-0.0031}$	12.7	13.0

$e^+e^- \to \tau^+\tau^-$			
Model	ϵ (TeV^{-2})	Λ^-(TeV)	Λ^+(TeV)
LL	$-0.0033^{+0.0056}_{-0.0050}$	8.9	11.4
RR	$-0.0036^{+0.0061}_{-0.0056}$	8.4	10.9
VV	$-0.0012^{+0.0017}_{-0.0020}$	14.0	19.1
AA	$-0.0004^{+0.0025}_{-0.0027}$	13.1	14.2
LR	$-0.0053^{+0.0079}_{-0.2210}$	2.1	9.2
RL	$-0.0053^{+0.0079}_{-0.2210}$	2.1	9.2
V0	$-0.0011^{+0.0023}_{-0.0033}$	12.3	15.7
A0	$-0.0028^{+0.0041}_{-0.0043}$	9.3	12.9

$e^+e^- \to l^+l^-$			
Model	ϵ (TeV^{-2})	Λ^-(TeV)	Λ^+(TeV)
LL	$-0.0042^{+0.0027}_{-0.0028}$	9.8	16.5
RR	$-0.0046^{+0.0037}_{-0.0034}$	9.4	15.8
VV	$-0.0014^{+0.0012}_{-0.0012}$	16.5	26.2
AA	$-0.0018^{+0.0016}_{-0.0019}$	14.0	21.7
LR	$-0.0023^{+0.0051}_{-0.0045}$	8.5	11.2
RL	$-0.0023^{+0.0051}_{-0.0045}$	8.5	11.2
V0	$-0.0020^{+0.0016}_{-0.0019}$	13.5	22.9
A0	$-0.0011^{+0.0025}_{-0.0023}$	13.2	15.6

Table 11: Fitted values of ϵ and 95% confidence limits on the scale, Λ, for constructive (+) and destructive interference (−) with the Standard Model, for the contact interaction models discussed in the text. Results are given for $e^+e^- \to \mu^+\mu^-$, $e^+e^- \to \tau^+\tau^-$ and $e^+e^- \to \ell^+\ell^-$, assuming universality in the contact interactions between $e^+e^- \to \mu^+\mu^-$ and $e^+e^- \to \tau^+\tau^-$.

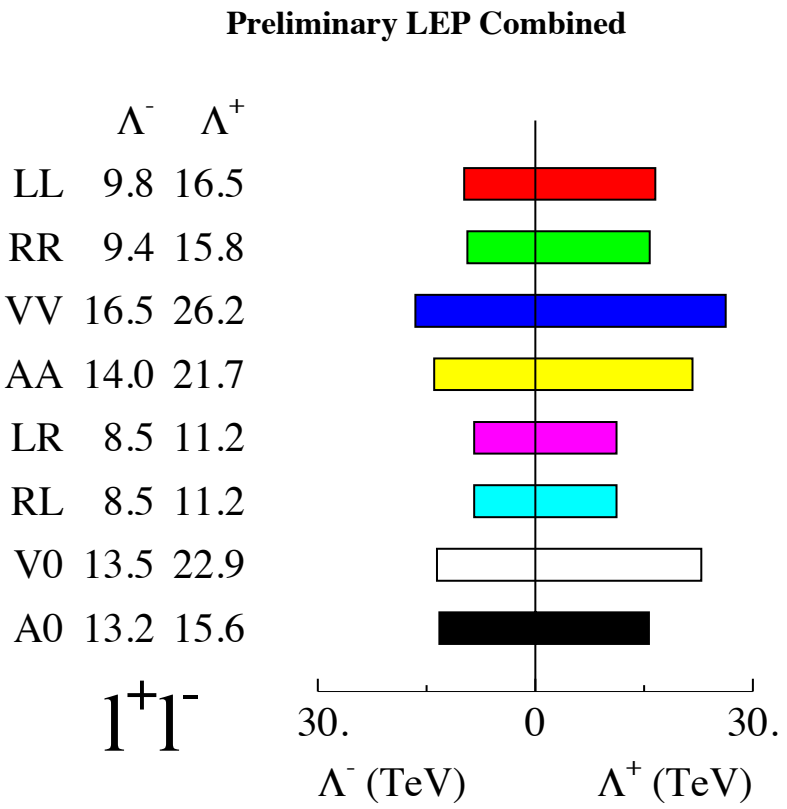

Figure 7: The limits on Λ for $e^+e^- \to \ell^+\ell^-$ assuming universality in the contact interactions between $e^+e^- \to \mu^+\mu^-$ and $e^+e^- \to \tau^+\tau^-$.

interactions.

6 Summary

A preliminary combination of the LEP-II $e^+e^- \to f\bar{f}$ cross-sections (for hadron, muon and tau final states) and forward-backward asymmetries (for muon and tau final states) from LEP running at energies from 130 to 207 GeV has been made. The results from the four LEP experiments are in good agreement with each other.

The averages for all energies are shown given in Table 2. Overall the data agree with the Standard Model predictions of ZFITTER, although the combined hadronic cross-sections are on average 1.8 standard deviations above the predictions. Further information is available at [5].

Preliminary differential cross-sections, $\frac{d\sigma}{d\cos\theta}$, for $e^+e^- \to \mu^+\mu^-$ and $e^+e^- \to \tau^+\tau^-$ were combined. Results are shown in Figures 3 and 4.

A preliminary average of results on heavy flavour production at LEP-II has also been made for measurements of R_b, R_c, $A_{FB}^{b\bar{b}}$ and $A_{FB}^{c\bar{c}}$, using results from LEP centre-of-mass energies from 130 to 207 GeV. Results are given in Table 7 and shown graphically in Figures 5 and 6. The results are in good agreement with the predictions of the SM.

The preliminary averaged cross-section and forward-backward asymmetry results together with the combined results on heavy flavour production were interpreted in a variety of models. The LEP-II averaged cross-sections were used to obtain lower limits on the mass of a possible Z' boson in different models. Limits range from 436 to 1890 GeV depending on the model. Limits on the scale of contact interactions between leptons and also between electrons and $b\bar{b}$ and $c\bar{c}$ final states have been determined. A full set of limits are given in Tables 11 and 12.

Acknowledgements

The analysis and interpretation of the high energy $f\bar{f}$ data requires the theoretical input from Monte Carlo programs to compute efficiencies, from programs to compute the luminosity and programs which make Standard Model predictions. We would like to acknowledge the work of all the authors of these programs. In particular we are grateful to D. Bardin, S. Jadach, G. Passarino and B. Ward for their direct contributions to our work.

$e^+e^- \to b\bar{b}$			
Model	ϵ (TeV^{-2})	Λ^-(TeV)	Λ^+(TeV)
LL	$-0.0030^{+0.0045}_{-0.0047}$	9.3	11.8
RR	$-0.1755^{+0.1634}_{-0.0159}$	2.2	7.7
VV	$-0.0029^{+0.0038}_{-0.0040}$	10.0	13.3
AA	$-0.0018^{+0.0029}_{-0.0031}$	11.6	14.6
LR	$-0.0491^{+0.0555}_{-0.0384}$	3.1	5.5
RL	$0.0065^{+0.1409}_{-0.0149}$	7.0	2.5
V0	$-0.0021^{+0.0032}_{-0.0034}$	11.0	13.9
A0	$0.0305^{+0.0203}_{-0.0348}$	6.4	4.0

$e^+e^- \to c\bar{c}$			
Model	ϵ (TeV^{-2})	Λ^-(TeV)	Λ^+(TeV)
LL	$0.0146^{+0.5911}_{-0.0259}$	5.3	1.3
RR	$0.0492^{+0.3723}_{-0.0568}$	4.6	1.5
VV	$0.0008^{+0.0106}_{-0.0100}$	7.4	6.7
AA	$0.0081^{+0.0171}_{-0.0154}$	6.6	5.0
LR	$0.0913^{+0.1076}_{-0.1251}$	3.5	2.1
RL	$0.0145^{+0.0872}_{-0.0872}$	2.9	2.6
V0	$0.0047^{+0.0170}_{-0.0133}$	6.9	1.4
A0	$0.0524^{+0.0736}_{-0.0780}$	4.0	2.6

Table 12: Fitted values of ϵ and 95% confidence limits on the scale, Λ, for constructive (+) and destructive interference (−) with the Standard Model, for the contact interaction models discussed in the text. From combined $b\bar{b}$ and $c\bar{c}$ results with centre of mass energies from 133 to 207 GeV.

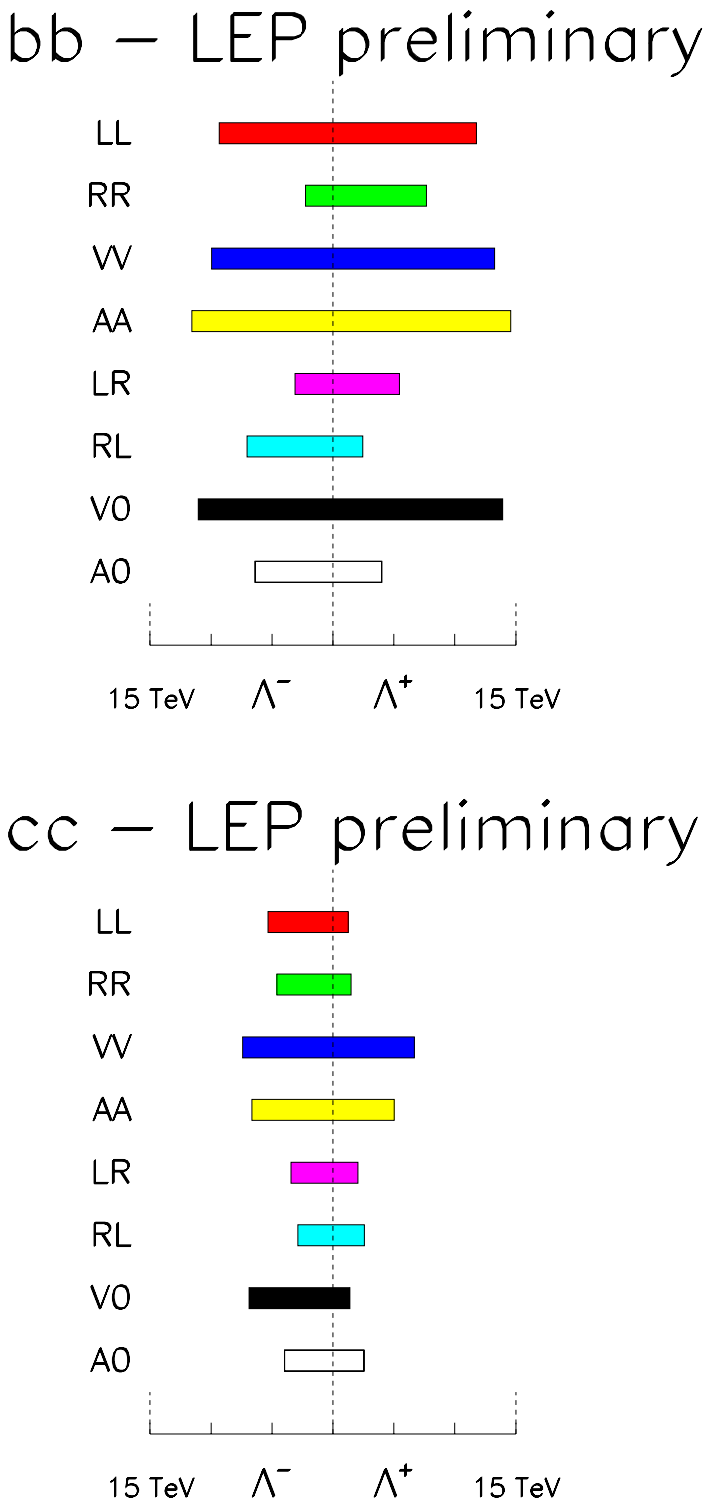

Figure 8: The 95% CL limits on the scale of Contact Interactions in $e^+e^- \to b\overline{b}$ and $e^+e^- \to c\overline{c}$ using Heavy Flavour LEP combined results from 133 to 207 GeV.

References

[1] LEPEWWG $f\bar{f}$ Subgroup, D. Bourilkov *et. al.*, LEP2FF/01-01,ALEPH 2001-039 PHYSIC 2000-013, DELPHI 2001-108 PHYS 896, L3 note 2663, OPAL TN690.

[2] LEPEWWG $f\bar{f}$ Subgroup, C. Geweniger *et. al.*, LEP2FF/00-03,ALEPH 2000-088 PHYSIC 2000-034, DELPHI 2000-168 PHYS 881, L3 note 2624, OPAL TN673.

[3] LEPEWWG $f\bar{f}$ Subgroup, D. Bourilkov *et. al.*, LEP2FF/00-01,ALEPH 2000-026 PHYSIC 2000-005, DELPHI 2000-046 PHYS 855, L3 note 2527, OPAL TN647.

[4] LEPEWWG $f\bar{f}$ Subgroup, D. Bourilkov *et. al.*, LEP2FF/99-01,ALEPH 99-082 PHYSIC 99-030, DELPHI 99-143 PHYS 829, L3 note 2443, OPAL TN616.

[5] LEPEWWG $f\bar{f}$ subgroup: http://www.cern.ch/LEPEWWG/lep2/ .

[6] ALEPH Collaboration "Study of Fermion Pair Production in e^+e^- Collisions at 130-183 GeV", Eur. Phys. J. **C12** (2000) 183;
ALEPH Collaboration, "Fermion Pair Production in e^+e^- Collisions at 189 GeV and Kimits on Physics Beyond the Standard Model", ALEPH 99-018 CONF 99-013;
ALEPH Collaboration, "Fermion Pair Production in e^+e^- Collisions from 192 to 202 GeV", ALEPH 2000-025 CONF 2000-021;
ALEPH Collaboration, "Fermion Pair Production in e^+e^- Collisions at high energy and Limits on Physics beyond the Standard Model ", ALEPH 2001-019 CONF 2001-016;
DELPHI Collaboration,"Measurement and Interpretation of Fermion-Pair Production at LEP energies from 130 to 172 GeV", Eur. Phys. J. **C11** (1999), 383;
DELPHI Collaboration, "Measurement and Interpretation of Fermion-Pair Production at LEP Energies from 183 to 189 GeV", Phys.Lett. **B485** (2000), 45;
DELPHI Collaboration, "Results on Fermion-Pair Production at LEP running from 192 to 202 GeV", DELPHI 2000-128 OSAKA CONF 427;
DELPHI Collaboration, "Results on Fermion-Pair Production at LEP running in 2000", DELPHI 2001-094 CONF 522;
L3 Collaboration, "Measurement of Hadron and Lepton-Pair Production at 161 GeV $< \sqrt{s} <$ 172 GeV at LEP", Phys. Lett. **B407** (1997) 361;
L3 Collaboration, "Measurement of Hadron and Lepton-Pair Production at 130 GeV $< \sqrt{s} <$ 189 GeV at LEP", Phys. Lett. **B479** (2000), 101.
L3 Collaboration, "Preliminary L3 Results on Fermion-Pair Production in 1999", L3 note 2563;
L3 Collaboration,"Preliminary L3 Results on Fermion-Pair Production in 2000", L3 note 2648;
OPAL Collaboration, "Tests of the Standard Model and Constraints on New Physics from Measurements of Fermion Pair Production at 130 - 172 GeV at LEP", Euro. Phys. J. **C2** (1998) 441;
OPAL Collaboration, "Tests of the Standard Model and Constraints on New Physics from Measurements of Fermion Pair Production at 183 GeV at LEP", Euro. Phys. J. **C6** (1999) 1;
OPAL Collaboration, "Tests of the Standard Model and Constraints on New Physics from Measurements of Fermion Pair Production at 189 GeV at LEP", Euro. Phys. J. **C13** (2000) 553;
OPAL Collaboration, "Tests of the Standard Model and Constraints on New Physics from Measurements of Fermion Pair Production at 192-202 GeV at LEP", OPAL PN424 (2000);

OPAL Collaboration, "Measurement of Standard Model Processes in e+e- Collisions at sqrts 203-209 GeV", OPAL PN469 (2001).

[7] D. Bardin *et al.*, CERN-TH 6443/92; http://www.ifh.de/∼riemann/Zfitter/zf.html .
Predictions are from ZFITTER versions 6.04 or later.
Definition 1 corresponds to the ZFITTER flags FINR=0 and INTF=0; definition 2 corresponds to FINR=0 and INTF=1 for hadrons, FINR=1 and INTF=1 for leptons.

[8] G. Montagna *et al.*, Comput. Phys. Commun. **117** (1999) 278.

[9] S. Jadach *et al.*, http://home.cern.ch/∼jadach/KKindex.html .

[10] L. Lyons *et al.*, Nucl. Inst. Meth. **A270** (1988) 110.

[11] M. Kobel *et al.*, "Two-Fermion Production in Electron Positron Collisions" in S. Jadach *et al.* [eds] , "Reports of the Working Groups on Precision Calculations for LEP2 Physics: proceedings" CERN 2000-009, hep-ph/0007180.

[12] ALEPH Collaboration, Euro. Phys J. **C12** (2000) 183;
DELPHI Collaboration, P.Abreu *et al.*, Euro. Phys J. **C11**(1999);
L3 Collaboration, M.Acciarri *et al.*, Phys. Lett. **B485** (2000) 71;
OPAL Collaboration, G.Abbiendi *et al.*, Euro. Phys. J. **C16** (2000) 41.

[13] ALEPH Collaboration, ALEPH 99-018 CONF 99-013;
ALEPH Collaboration, ALEPH 2000-046 CONF 2000-029;
DELPHI Collaboration, DELPHI 2001-095 CONF 523;
L3 Collaboration, L3 Internal note 2640, 1 March 2001.

[14] LEPEWWG Heavy Flavour at LEP2 Subgroup, "Combination of Heavy Flavour Measurements at LEP2", LEP2FF/00-02.

[15] ZFITTER V6.23 is used.
D. Bardin *et al.*, Preprint hep-ph/9908433.
Relevant ZFITTER settings used are FINR=0 and INTF=1.

[16] DELPHI Collaboration, P.Abreu *et al.*, Euro Phys J. **C10**(1999) 415.
The LEP collaborations *et al.*, CERN-EP/2000-016.

[17] P. Langacker, R.W. Robinett and J.L. Rosner, Phys. Rev. **D30** (1984) 1470;
D. London and J.L. Rosner, Phys. Rev. **D34** (1986) 1530;
J.C. Pati and A. Salam, Phys. Rev. **D10** (1974) 275;
R.N. Mohapatra and J.C. Pati, Phys. Rev. **D11** (1975) 566.

[18] G. Altarelli *et al.*, Z. Phys. **C45** (1989) 109;
erratum Z. Phys. **C47** (1990) 676.

[19] DELPHI Collaboration, P. Abreu *et al.*, Zeit. Phys. **C65** (1995) 603.

[20] E. Eichten, K. Lane, and M. Peskin, Phys. Rev. Lett. **50** (1983) 811.

[21] H. Kroha, Phys. Rev. **D46** (1992) 58.